Desalination and Water Treatment
www.deswater.com

doi:10.5004/dwt.2017.11373

69 (2017) 123–129
March

IEX and BMED hybrid process for dilute organic acids recovery: identification of key steps to manage energy consumption

M. Jaouadi[a,b], J. Ding[a], A. Hannachi[b,*], L. Muhr[a]

[a]*LRGP, ENSIC-CNRS, 1 rue Grandville, BP 20451, 54001 NANCY Cedex France, Tél. +33 3 83 17 53 11; Fax: +33 3 83 32 29 75; email: laurence.muhr@univ-lorraine.fr*
[b]*GPSI, National Engineering School of Gabes, University of Gabes, Street of Omar Ibn El Khattab, 6029 Gabes, Tunisia, Tel. +216 75392100; Fax: +216 75392190; email: ahmed.hannachi@enig.rnu.tn*

Received 20 April 2016; Accepted 1 June 2016

ABSTRACT

Recently, several research works highlighted the interest of hybrid separation process combining bipolar membrane electrodialysis (BMED) and ion exchange (IEX) for the recovery and concentration of organic acids from diluted effluents. The mechanisms involved in such hybrid systems are numerous. They include: transfer through ion exchange membranes, transport within aqueous solution, transport within ion exchange resin bed, and water dissociation within bipolar membranes. The present work aims at getting a better understanding of the mechanisms involved in this hybrid system and at proposing a methodology to minimize energy consumption as function of the required purity or concentration factor. For this purpose, an experimental investigation was carried out on a BMED-IEX hybrid pilot unit with different types of IEX resins. Experimental measurements conducted, consecutively with decoupled and coupled systems, allowed evaluating the contribution of each step in the overall energy consumption. The approach allowed as well identifying what would be the concentration factor to reduce energy consumption.

Keywords: Bipolar membrane electrodialysis (BMED); Ion exchange resins (IEX); Hybrid separation process; Organic acid recovery; Energy consumption

1. Introduction

Organic acids have many applications for our daily life products such as: food, drugs, cosmetics, detergents. They can be produced by chemical synthesis, but in green chemistry context, fermentations or transformations of biomass are more interesting pathways. Organic acids produced are also a source of building-block molecules for the manufacture of bio-based products. Such application usually requires high purity acids, leading to the need for developing adapted separation techniques. Another area where organic acids separation is an important issue regards the development of "integrated" fermentation processes either for organic acids production or for the removal of inhibitory compounds during fermentation process [1–5]. The recovery of carboxylic acids in aqueous effluents is an additional environmental challenge for industries using acids [6]. For instance carboxylic acids are by-products of many industrial processes. Their recovery allows decreasing water COD contents to satisfy discharge requirements and possibly valorization of dilute effluents as useful concentrated solutions. Treatment of very low organic acid concentrations in solutions could pose specific challenges. For all these applications, separation unit operations play a major role. Separation and purification of organic acids from complex matrices, in which they are often highly diluted, is a defying task. Among the arsenal of separation techniques available, electro-membrane processes are of particular interest

*Corresponding author.

Presented at the EDS conference on Desalination for the Environment: Clean Water and Energy, Rome, Italy, 22–26 May 2016.

for environmental reasons. A state of the art on the use of such processes was described by Huang et al. [7], where the authors highlighted the development of many electro dialysis-based architectures for organic acids production. These architectures result often of the hybridization of several techniques. In a non-exhaustive way, these techniques include: conventional electrodialysis (ED), bipolar membrane electrodialysis (BMED), electro-electrodialysis (EED), electrodeionization (EDI). In the case of fermentation media treatment, approaches sometimes integrate a pretreatment step which is often nanofiltration [8]. Regarding architectures which involve bipolar membranes, their ability to produce H^+ and OH^- thanks to water dissociation justifies their great potential for environmentally friendly applications [9]. In the literature, several methodologies were proposed to assess BMED cost and energy consumption [10]. These approaches also intended to compare the costs of different types of separation processes [11].

Our study focuses on hybridization of BMED and ion exchange (IEX). While many investigations regarding the production of high-purity water were carried out using electrodialysis-ion exchange hybridization, only few focused on dealing with organic acid production. Among works related to organic acids production, Widisia et al. [12] studied the use of conventional electrodialysis/ion exchange for citric acid production. Zhang et al. [13] used BMED/IEX for tartaric acid production. Both studies highlighted the interesting performances of such hybrid processes.

The present work is an extension of a previous investigation meant to treat dilute acetic acid solutions through a hybrid BMED/IEX allowing recovering concentrated organic acid solutions [1]. The former study highlighted the interest of the hybridization for this application. The current work aims at getting a better understanding of the numerous mechanisms involved in the system. An experimental investigation has been conducted to evaluate the contribution of each step in the overall energy consumption. This methodology relied on measurements carried out successively with decoupled and coupled systems. This approach also intends to unfold the main sources of energy consumption allowing implementing procedures favoring energy savings.

2. Materials and methods

2.1. Experimental set-up

The experimental set-up, used in this work, is a 'filter press' type stack which was built by LRGP workshop. The device is illustrated in Fig. 1. It includes from left to right: electrolyte compartment (N°1), bipolar membrane (BM), dilution compartment in which circulates batch-wise a solution from which acetic acid is to be removed (N°2), anionic membrane (AMX) through which acetate ions are transferred, concentration compartment where acetic acid is recovered (N°3), bipolar membrane and electrolyte compartment. Both organic acid compartments have a thickness of 1.5 cm. Membrane exchange area is 2 × 20 cm^2. Dilution compartment is filled with either strong or weak anion exchange resins initially under acetate form. However, the concentration compartment is optionally filled with strong cationic exchange resins under H^+ form.

Several transport mechanisms occur within the system: transfer through ion exchange membranes, transport within aqueous solution, transport within ion exchange resin bed, and water dissociation within bipolar membranes. In order to evaluate the contribution of each step on the overall energy consumption, experiments were conducted consecutively with "decoupled" systems illustrated in Figs. 2–5. System illustrated in Fig. 2 involves only the electrolytic compartments. Systems illustrated in Figs. 3 and 4 involve the electrolytic compartments and respectively anionic membrane (Fig. 3) and bipolar membrane (Fig. 4). System illustrated in Fig. 5 is close to the complete one (Fig. 1), the difference being the absence of cationic resins in concentration compartment (N°3).

2.2. Products, ion-exchange resins and membranes

Chemicals were purchased from Sigma-Aldrich: Sodium sulfate (Na_2SO_4), sodium hydroxide (NaOH) and acetic acid (CH_3COOH) have purity respectively higher than 99%, 98% and 99%. Ion exchange resins were also purchased from Sigma-Aldrich. Their properties are given in Table 1. The membranes were purchased from Eurodia. Membranes' properties are summarized in Table 2.

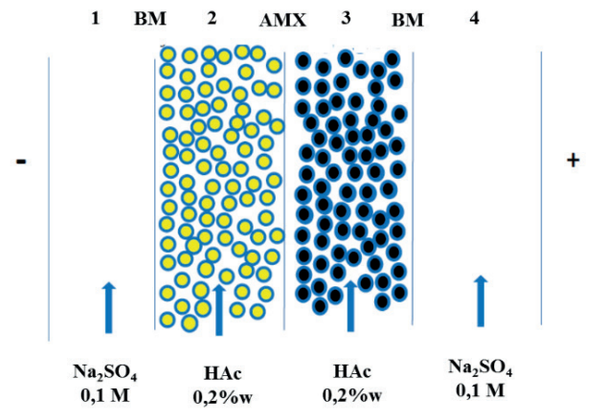

Fig. 1. Schematic representation of the "complete" EDMB-IEX stack.

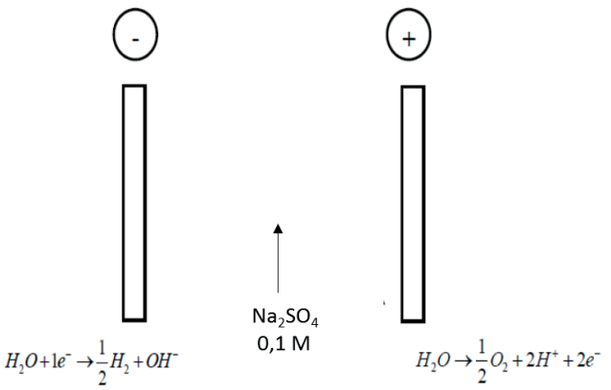

Fig. 2. System involving only electrolytic compartments (N°1 and N°4 in Fig. 1).

2.3. Materials and analytical methods

A Sorensen DCS 150-7E (150V-7A) generator was used for imposing the electric current through the stack. It can operate either in galvanostat or in potentiostat mode. Galvanostat mode was used in the present work. Solutions acidity was measured using a Symphony SC80PC VWR pH meter. Conductivity measurements were carried out by means of a Meterlab (Radiometer analytical) CDM210 conductimeter (detection range: 1–999.9 µS/cm).

3. Results and discussion

3. 1. Evaluation of the resistive contributions of the stack elements

3.1.1. Electrolyte compartments resistance, R_{EC}

Voltage was measured as a function of current using the system illustrated in Fig. 2. Results are presented in Fig. 6. A fairly good linear relationship between voltage, U, and current, I, was obtained ($R^2 = 0.971$):

$$U = 4.5958\, I + 2.10 \quad (1)$$

Voltage across the cell stack can be expressed as follows:

$$U_{Cell} = U_0 + \eta_a + |\eta_c| + U_{Ohm} \quad (2)$$

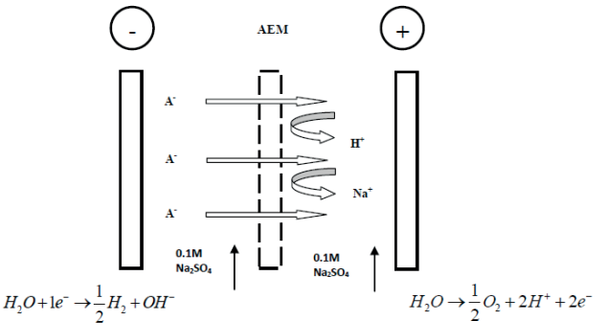

Fig. 3. System involving electrolytic compartments and anionic membrane.

where U_0 is the cell voltage at zero current, η_a and η_c are the anode and cathode overvoltage and U_{Ohm} represents the Ohmic drop. Assuming that current lines are perpendicular to the electrodes, the latter could be obtained by the following expression:

$$U_{Ohm} = R_{EC} I \quad (3)$$

Identification of terms in Eqs. (1) and (2), allows concluding that: $U_0 + \eta_a + |\eta_c| = 2.10$ V and the resistance of the two electrolytic compartments, R_{EC}, is:

$$R_{EC} \approx 4.60\ \Omega \quad (4)$$

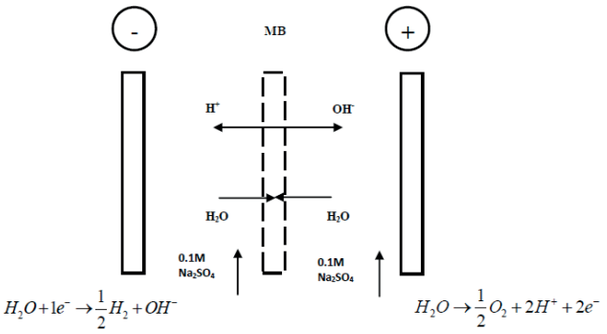

Fig. 4. System involving electrolytic compartments and bipolar membrane.

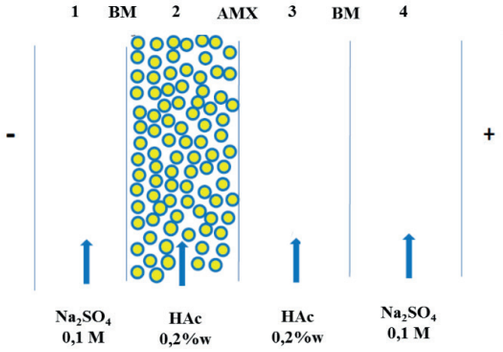

Fig. 5. Schematic representation of the EDMB-IEX stack with anionic resin (weak or strong) in the dilution compartment.

Table 1
Ion exchange resins' properties

Resins	Matrix	Structure	Capacity	Particle size
DIAION WA30	Anionic Weakly basic Macroreticular	Styrene-DVB Functional group: dimethyl amine	Free base form > 1.5 eq/L	Average: 470 µm
AMBERSEP 900 OH	Anionic Strongly basic Macroreticular	Styrène-DVB Functional group: Type 1 quaternary ammonium	> 0.8 eq/L	300–750 µm
AMBERLITE IRN77	Cationic Strongly acidic Gel	Styrene-DVB Functional group: sulfonic acid	≥ 1.90 eq/L	600–700 µm

Table 2
Membranes' properties

Membrane type	Nature	Characteristic	Thickness (mm)	Electric resistance[a] (Ωcm^2)
AMX (Neosepta)	Strongly basic	High mechanical strength	0.12–0.18	2.0–3.5
BP (Tokuyama Soda)	Bipolar	–	200–350	–

[a]Electric resistance: equilibrated with 0.5 N NaCl solution, at 25°C.

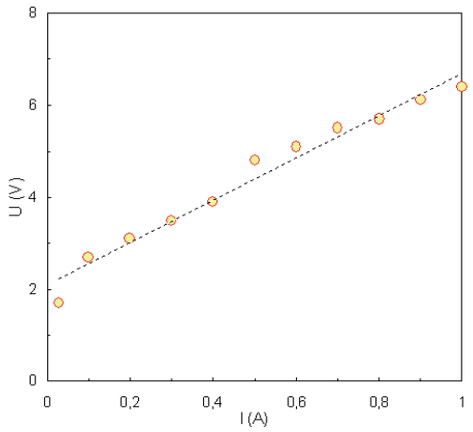

Fig. 6. Voltage across the cell stack vs. current using system illustrated in Fig. 2 (electrolytic compartments).

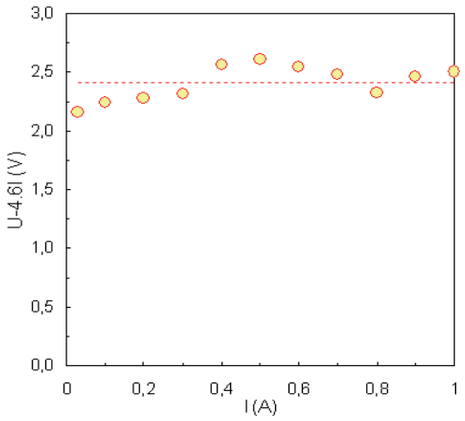

Fig. 7. [U_{cell} – 4.6 I] vs. I (Experiments carried out using system illustrated in Fig. 4).

3.1.2. Anionic membrane resistance, R_{AMX}

A similar approach was carried out using the system illustrated in Fig. 3. An affine relationship between voltage and current was obtained (R^2 = 0.987):

$$U = 4.6319\, I + 2.10 \tag{5}$$

Overall cell resistance is the sum of the resistances of each element constituting the stack. In this case electrolytic compartment resistance is added to the anionic membrane resistance:

$$R_{Cell} = R_{EC} + R_{AMX} \tag{6}$$

where R_{EC} is the resistance of the electrolytic compartments previously defined and R_{AMX} is the resistance of the anionic membrane. The latter could be derived using Eqs. (1) and (5), leading to:

$$R_{AMX} = 0.036\ \Omega \tag{7}$$

It must be noticed that the contribution of anionic membrane in overall resistance is very low compared to other contributions. Because of lack of precision, this value of R_{AMX} must be considered as an order of magnitude. In fact it could be compared to the one calculated using membrane properties given in Table 2 (corresponding to 0.5 N NaCl solutions). As membrane area is 2 × 20 cm^2, R_{AMX} would be in the range of 0.05 and 0.09 Ω. Despite lack of precision and although it was obtained under different conditions, the experimental resistance is close to the expected range previously defined. In the following part of this work and although the solution which is in contact with the membrane could be different (acetic acid 0.2%w), the value for R_{AMX} given by Eq. (7) will be considered.

3.1.3. Bipolar membrane resistance, R_{BM}

Voltage was measured as a function of current using the system illustrated in Fig. 4. In order to explain the methodology used to determine bipolar membrane resistance, theoretical expression of this resistance can be reminded [10]:

$$R_{BM} = \frac{2.3RT\Delta pH}{IF} \tag{8}$$

where R is the ideal gas constant, T is the absolute temperature, ΔpH is the pH difference between solutions in contact with both sides of the bipolar membrane, I is the current and F is the Faraday constant. R_{BM} is therefore inversely proportional to I.

Taking into account resistances additivity, voltage across the cell stack is given by:

$$U_{cell} = \left[U_0 + \eta_a + \left|\eta_c\right|\right] + \left(\frac{2.3RT\Delta pH}{F} + R_{EC}I\right) \tag{9}$$

In order to evaluate bipolar membrane contribution, (U_{cell} – 4.6 I) was calculated and presented as function of current in Fig. 7.

It can be observed that [$U_{cell} - 4.6\,I$] vs. I does not exhibit any significant variation and can therefore be regarded as constant with an average value of 2.41 V. Thus, the bipolar membrane contribution is: 0.31 V.

A theoretical value for this voltage can be estimated using Eq. (8) with T = 295.15 K and the measured ΔpH for the configuration illustrated in Fig. 1. The pH difference between solutions on both sides of the bipolar membrane corresponds to the difference between a neutral pH for Na_2SO_4 electrolyte solution and the pH of the acetic acid solution (0.2%w). The pH difference across the membrane is 7–3.1 = 3.9 giving a contribution of the bipolar membrane of 0.23 V. This value is slightly lower than the experimental one. Despite the differences between the configurations illustrated in Figs. 1 and 4, close values of cross membrane voltage were obtained. Part of the discrepancies could be also attributed to experimental errors.

In the following part of this work, R_{BM}, will be estimeted using the following equation:

$$R_{BM} = \frac{0.31}{I} \tag{10}$$

3.1.4. Dilution and concentration compartments' resistances

For determining dilution and concentration compartments' resistances, a different protocol from the previous ones has been implemented. Systems illustrated in Figs. 1 and 5 were used. Two acetic acid solutions having an initial concentration 0.2% w (0.033 M) were allowed to separately flow through dilution (N°2) and concentration (N°3) compartments. In each compartment 2 L of solution circulated batch wise with a flow rate of 42 mL/min. *A* constant current I = 0.5 A, corresponding to 12.5 mA/cm² current density was applied.

Variation of voltage across the cell stack as a function of time is illustrated in Fig. 8 for four configuration types:

- Points noted af and AF correspond to the system illustrated in Fig. 5. Notation af is used for weak anionic resins DIAION WA30 whereas AF denotes strong anionic resins AMBERSEP 900.
- Points noted af + CF and AF + CF correspond to the system illustrated in Fig. 1 where CF denotes the strong cationic resins Amberlyst IRN77. These resins were under H^+ form.

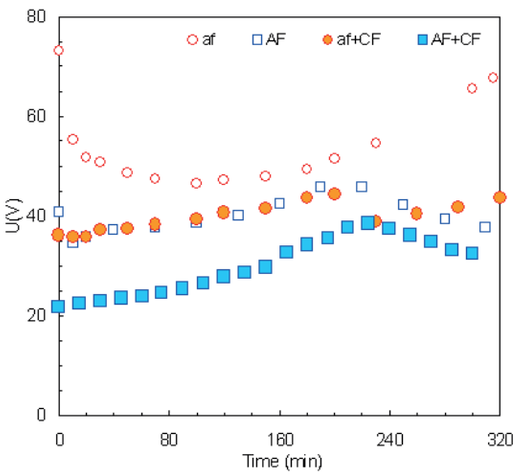

Fig. 8. Variation of voltage across the cell stack vs. time (systems illustrated in Figs. 1 and 5).

To compare the ohmic drops obtained with the different systems, it is necessary to consider stable operation of the treatment cell. The notion of stabilization will be later discussed in this article. For the first 20 min of the treatment acetic acid concentrations in the dilution compartment were very similar (0.0305 ± 0.0015 M) regardless of the configuration type. After 20 min, voltages across the cell stack are given in Table 3 for the four configuration types.

Referring to Fig. 1, adding up resistances in series allows writing the following equation for the cell voltage:

$$U_{cell} = U_0 + \eta_a + |\eta_c| + I\,\Sigma R_i \tag{11}$$

where ΣR_i is the overall cumulative resistance within the cell stack, expressed by:

$$\Sigma R_i = R_{EC} + 2R_{BM} + R_{DC} + R_{AMX} + R_{CC} \tag{12}$$

R_{DC} and R_{CC} are the resistances of the dilution and concentration compartments respectively. Accounting for the previously assessed resistances (Eqs. (4), (7), (10) and (12)), the cumulative resistance of both concentration and dilution compartments, R_{D+C}, can be evaluated by:

$$R_{D+C} = R_{DC} + R_{CC} = \left(\frac{U_{cell} - 2.10}{I}\right) - \left(4.60 + 2 \times \frac{0.31}{I} + 0.036\right) \tag{13}$$

The values measured for this resistance are reported in Table 3. It can be noted that, as far as highly diluted solutions are concerned, the main resistive contribution is located in the compartments where acetic acid solution is flowing.

Differences of cumulative resistance between weak and strong anionic resins are 26.4 and 31.8 Ω with and without cationic resins in the concentration compartment, respectively. Despite uncertainty, it is clear that strong anionic resins bed in acetate form immersed in 0.0305 M acetic acid solution is more conductive than weak anionic resins bed. The results shown in the Table 3 indicate that, inserting cationic resins under H^+ in the concentration compartment

Table 3
Resistive contribution of dilution and concentration compartments

Configuration	af[a]	AF[a]	af + CF[a]	AF + CF[a]
U_{cell} (V)	51.7	35.8	35.8	22.6
ΣR_i (Ω)	103.4	71.6	71.6	45.2
R_{D+C} (Ω)	93.3	61.5	61.5	35.1

[a]af: Dilution compartment filled with weak anionic resins; AF: strong anionic resins in dilution compartment; af + CF: weak anionic resins in dilution compartment and strong cationic resins in concentration compartment; AF + CF: strong anionic resins in dilution compartment and strong cationic resins in concentration compartment.

led to much lower values for R_{D+C}. In fact the resistance dropped by 34% and 43% for weak and strong anionic resins in the dilution compartment, respectively.

In the considered time interval, average acetic acid concentration and conductivity in the concentration compartment are respectively 0.4588 M and 336 μS cm^{-1}. Knowing the transfer area, $S = 2 \times 20$ cm^2, and the compartment thickness, $e = 1.5$ cm, the concentration compartment resistance can be calculated using:

$$R = \frac{e}{S\kappa} \tag{14}$$

where κ is the solution conductivity. Eq. (14) predicts resistance values of 110 Ω and 90 for just the concentration compartment when weak and strong anionic resins are filling the dilution compartment, respectively. These figures are much higher than the cumulative resistances reported in Table 3. The differences could be explained by the fact that H^+ ions (and OH^- ions on the other membrane side) generated by bipolar membrane contribute to solution conductivity in the considered compartment. H^+ ions produced by bipolar membrane in compartment three migrate towards anionic membrane where Ac^- ions are transferred in the opposite direction. AcH form of this weak acid does not contribute to the solution conductivity. However, migration of these ions within the cell contributes to the solution conductivity. This emphasizes validity limits of Eq. (14) in compartments where H^+ or OH^- ions are generated by a bipolar membrane. In the absence of other laws the relationship given by Eq. (3) is often used to calculate EDMB energy consumption leading to overestimated values if contributions provided by H^+ (or OH^-) transfer are not taken into account.

H^+ and OH^- contribution can also be observed at the beginning of the experiment, when current is applied. High voltage value is initially obtained and, within few minutes, voltage decreases to reach what was previously qualified a "stabilized" regime. At start of the experiment, H^+ and OH^- which begin to be produced by bipolar membranes have not yet had time to contribute to the conductivity of the compartments.

3.2. Specific energy consumption

Results presented in this section were relative to experiments carried out using system illustrated in Fig. 1. Dilution compartment (N°2) is filled with strong anionic resins Ambersep 900 initially under Ac^- form whereas concentration compartment (N°3) is filled with strong cationic resin Amberlite IRN77 under H^+ form. The experimental protocol is identical to the one described in section 3.1.4.

Acetate transfer rate between the compartments can be determined by monitoring acetic acid concentration in compartment 2 or/and 3 accounting for conservation equations. Dilution compartment concentration and the number of transferred acetate moles variations with time are presented in Fig. 9. As expected, the transfer rate decreases as the solution in the dilution compartment gets depleted. As few acetate ions are available, current transport is provided by other ions, including OH^- generated by bipolar membrane. Energy is then consumed for a transfer of other species than the desired one.

The variation with acid concentration in the dilution compartment of the specific energy consumption, expressed in kWh per kg of acetic acid transferred, is showing in Fig. 10. It can be observed that specific energy consumption increases as the solution concentration in the dilution compartment decreases. However, the increase becomes exponential for very low acetic acid concentrations in the dilution compartment. Thus, there is a time beyond which the transfer would be extremely energy consuming. It is very important to know when exactly the experiment should be stopped. In Fig. 9, it can be observed that desired transfer decreases when time exceeds 200 min. For such treatment times, transfer becomes predominantly that of OH^- ions. In Fig. 8, during this time interval, in the AF + CF system configuration voltage passes through a maximum and then decreases. When acetic acid concentration in dilution compartment is low, proportion of OH^- ions which react with acetic acid to give acetate ions is low as well. Transport is then mostly provided by OH^- ions which have higher ionic conductivity than acetate ($\lambda(OH^-) = 198\ 10^{-4}$ m^{2}S mol^{-1} while $\lambda(Ac^-) = 40.9\ 10^{-4}$ m^{2}S mol^{-1} [14]). This leads to voltage decrease. For this issue, the begin-

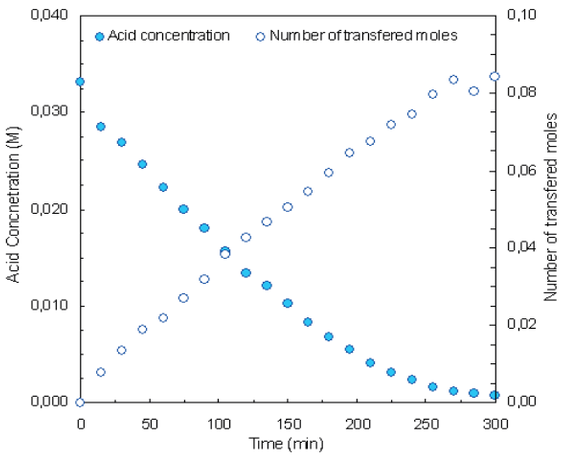

Fig. 9. Acetic acid concentration in the dilution compartment (N°2) and number of transferred moles vs. time (configuration AF + CF).

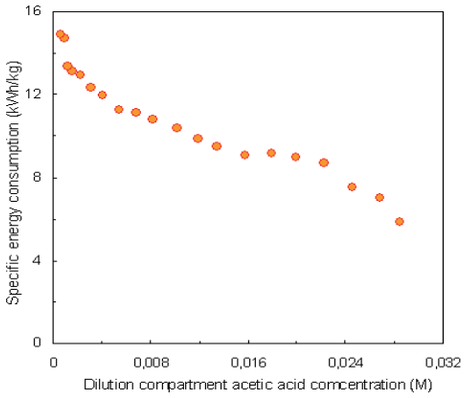

Fig. 10. Specific energy consumption (kWh/kg of acetic acid transferred) vs. final acid concentration in the dilution compartment (initial concentration: 0.033 M).

ning of voltage decrease indicates therefore, when to stop the system. It should also be noticed that, if experiments are further continued, OH^- generation leads to alkalinity increase. A high pH, caused by polarization concentration in the anionic membrane vicinity may lead to a color change of the membrane. Therefore, the recommended pH interval of AMX membranes use should be respected.

4. Conclusion

In order to reduce acetic acid concentration in diluted effluents and to recover a concentrated fractions, a hybrid system involving BMED and ion exchange resins in the dilution compartment (anionic resin), and optionally in the concentrating compartment (strong cationic resin under H^+ form), was implemented.

Assessment of the resistive contribution of components of the stack has been carried out on consecutively decoupled and coupled systems led to the following results:

- As far as highly diluted (0.2%w acetic acid) weak acids are concerned, the main resistive contribution is located at the level of the compartments in which circulates acetic acid.
- H^+ and OH^- ions generated by bipolar membranes contribute to the conductivity of the compartments where these ions are released. The conductivity of the solution which circulates through this compartment cannot be solely considered for predicting resistance values.
- Specific energy consumption strongly depends on the desired final concentration of acid. Monitoring the voltage across the stack enabled to determine the time at which it is appropriate to stop the treatment to avoid additional energy consumption for unworthy other species than acetate ions.

Acknowledgements

This research was partially supported by the Energy and Environment Carnot Institute of Lorraine.

References

[1] A. Rehouma, B. Belaissaoui, A. Hannachi, L. Muhr, Bipolar membrane electrodialysis and ion exchange hybridizing for dilute organic acid solutions treatment, Desal. Wat. Treat., 51 (2013) 511–517.
[2] M.-t. Gao, M. Hirata, M. Koide, H. Takanashi, T. Hano, Production of L-lactic acid by electrodialysis fermentation (EDF), Process Biochem., 39 (2004) 1903–1907.
[3] M.-t. Gao, M. Koide, R. Gotou, H. Takanashi, M. Hirata, T. Hano, Development of a continuous electrodialysis fermentation system for production of lactic acid by *Lactobacillus rhamnosus*, Process Biochem., 40 (2005) 1033–1036.
[4] J.S. Tan, R.N. Ramanan, T.C. Ling, M. Shuhaimi, A.B. Ariff, Enhanced production of periplasmic interferon alpha -2b by *Escherichia coli* using ion-exchange resin for *in-situ* removal of acetate in the culture, Biochem. Eng. J., 58–59 (2011) 124–132.
[5] J.S. Tan, T.C. Ling, M. Shuhaimi, Y.J. Tam, R.N. Ramanan, A.B. Ariff, An integrated bioreactor-expanded bed adsorption system for the removal of acetate to enhance the production of alpha-interferon-2b by *Escherichia coli*, Process Biochem., 48 (2013) 551–558.
[6] A. Vertova, G. Aricci, S. Rondinini, R. Miglio, L. Carnelli, P. D'Olimpio, Electrodialytic recovery of light carboxylic acids from industrial aqueous waste, J. Appl. Electrochem., 39 (2009) 2051–2059.
[7] C. Huang, T. Xu, Y. Zhang, Y. Xue, G. Chen, Application of electrodialysis to the production of organic acids : State-of-the-art and recent development, J. Membr. Sci., 288 (2007) 1–12.
[8] M.J. Wozniak, K. Prochaska, Fumaric acid separation from fermentation broth using nanofiltration (NF) and bipolar electrodialysis (EDMB) Separ. Purif. Technol., 125 (2014) 179–186.
[9] C. Huang, T. Xu, Electrodialysis with bipolar membranes for sustainable development, Environ. Sci. Technol., 40 (2006) 5233–5243.
[10] H. Strathmann, G.H. Koops, Process Economics of Electrodialytic Water Dissociation for the Production of Acid and Base, Ed. A.J.B. Kemperman, Handbook on Bipolar Membrane Technology, Twente University Press, Enscheda, 2000, pp. 191–220.
[11] Y. Wang, C. Huang, T. Xu, Which is more competitive for production of organic acids, ion-exchange or electrodialysis with bipolar membranes? J. Membr. Sci., 374 (2011) 150–156.
[12] I.N. Widiasa, P.D. Sutrisna, I.G. Wenten, Performance of a novel electrodeionization technique during citric acid recovery, Separ. Purif. Technol., 39 (2004) 89–97.
[13] K. Zhang, M. Wang, D. Wang, C. Gao, The energy-saving production of tartaric acid using ion exchange resin-filling bipolar membrane electrodialysis, J. Membr. Sci., 341 (2009) 246–251.
[14] D.R Lide, H.P.R. Frederikse, CRC Handbook of Chemistry and Physics, Ed. CRC Press Boca Raton, 74th Ed., Florida, 1993–1994.